ENGINEERING TRIPOS PART IB

Tuesday 6 June 2006 9.00 to 11.00

Paper 3

MATERIALS SOLUTIONS

1(a) A binary alloy is a mixture of two compositions, that can be either metals (e.g. Cu and Zn), metal and non-metal (e.g. Fe and C) or ceramics (e.g. MgO and Al_2O_3).
The Fe-C phase diagram contains examples of (i) - (iv).
(i) Solidus lines are phase boundaries that define the top of a 100% solid field and separate solid and solid + liquid (α / α + L and β / β + L) regions of the phase diagram.

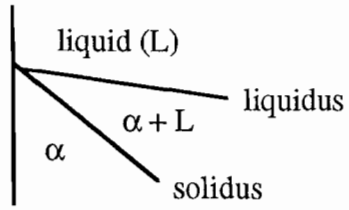

(ii) Liquidus lines are phase boundaries that define the bottom of a 100% liquid field and separate liquid and liquid + solid (L / α + L and L / β + L) regions of the phase diagram.

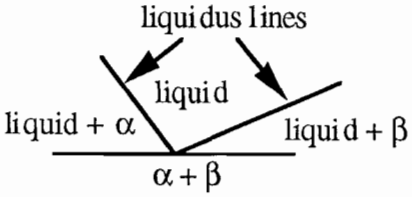

(iii) The eutectoid point represents the lower limit of the single-phase solid field formed by the intersection of the two solidus lines (e.g. at a composition of 0.8 wt % C and 723°C in the Fe-C system). The solid γ is transformed reversibly into two solid phases (α and β) at the eutectoid temperature (i.e. the lowest temperature at which 100% single phase solid is stable) and composition.

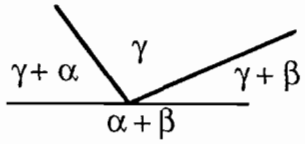

(iv) The eutectic point represents the lower limit of the single-phase liquid field formed by the intersection of the two liquidus lines. The liquid is transformed reversibly into two solid phases (α and β) at the eutectic temperature (i.e. the lowest temperature at which 100% liquid is stable) and composition.

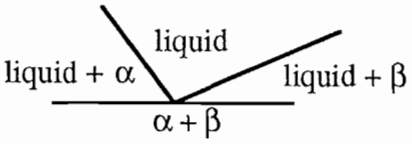

[2 marks for identifying features without explanation or example.] [6]

(b) The lever rule is used to calculate the mass (or weight) fraction of one particular phase in a two phase alloy of known net composition at a given temperature (i.e. constitution point) and is applied as follows;
1. A tie line is constructed across the two-phase region at the temperature of the alloy;
2. The overall alloy composition is located on the tie line;
3. The fraction of the phase at one end of the tie line is calculated by taking the length of the tie line from the overall alloy composition to the phase at the other end of the tie line and dividing by the total length of the tie line;
4. This method is only applicable for a phase diagram with weight or mass fraction on the abscissa scale.

Derivation of the lever rule is based on two conservation of mass expressions;
1. The sum of the mass fractions of the two phases in a two phase alloy must sum to unity;

$$W_\alpha + W_\beta = 1$$

where W_α and W_β are the mass fractions of each phase (α and β in this example).
2. The mass of one of the components that is present in both phases must be equal to the mass of that component in the total alloy;

$$W_\alpha C_\alpha + W_\beta C_\beta = C_0$$

where C_0 is the overall composition of that component in the alloy.

Solution of these simultaneous equations yields;

$$W_\alpha = \frac{C_0 - C_\beta}{C_\alpha - C_\beta} \quad \text{and} \quad W_\beta = \frac{C_\alpha - C_0}{C_\alpha - C_\beta}, \text{ as required.}$$ [6]

(c) From Figure 6.2 in the Materials Data Book, the phases present at a constitution point of 30 wt % Sn, 70 wt % Pb and 200°C are the α phase (Sn) and a liquid phase. The compositions of these phases are determined as follows;
Plot this composition/temperature point on the phase diagram (shown below as B). The composition of each phase determined by constructing a tie line across the α + L phase field at 200°C as shown below. The composition of the α phase corresponds to the tie line intersection with the $\alpha/(\alpha+L)$ phase boundary - about 17 wt % Sn and 83 wt % Pb (denoted as C_α).

Similarly the liquid phase has composition approximately 56 wt % Sn and 44 wt % Pb.
Using the lever rule, the mass fractions W_α and W_L can be calculated as follows;

$$W_\alpha = \frac{C_L - C_0}{C_L - C_\alpha} = \frac{56 - 30}{56 - 17} = 0.67 = \mathbf{67\ wt\ \%\ (\pm\ 2\ wt.\%)}$$

$$W_L = \frac{C_0 - C_\alpha}{C_L - C_\alpha} = \frac{30 - 17}{56 - 17} = 0.33 = \mathbf{33\ wt\ \%\ (\pm\ 2\ wt.\%)}$$

Use of the lever rule by measuring fractional lengths of a tie line is only valid for a linear wt. % scale. Wt. % does not vary linearly with atom % (which defines *molar* fractions), however, in which case the tie line lengths cannot be measured directly from the phase diagram. In this case it is necessary to add the corresponding non-linear wt. % scale along the top of the phase diagram and measure the actual wt. % values from the wt. % scale. [6]

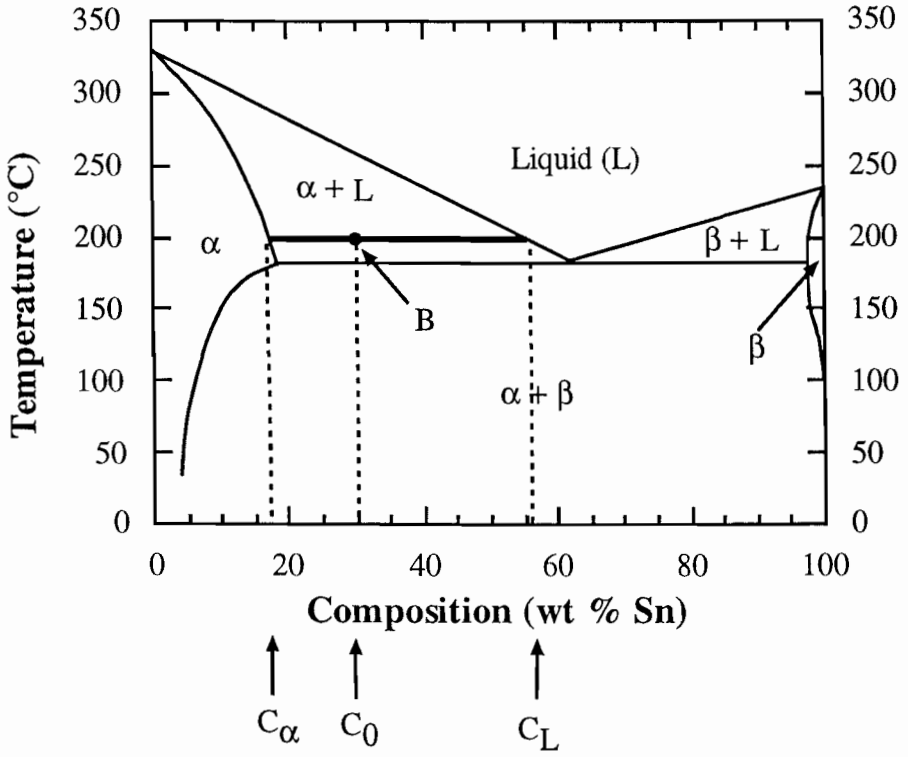

(d) 60 wt % Sn and 40 wt % Pb is the eutectic composition for this system, which has the lowest possible melting point (≈ 185°C)/highest fluidity for a Sn-Pb alloy. This alloy is particularly useful as a solder (since it is easily melted) for electronic applications, where it is desirable to minimise the heat input into individual devices. [2]

2 (a) A ceramic (from keramos; the Greek word for heat) is a complex polycrystalline inorganic compound of metal and non-metal elements or non-metal and non-metal elements such as alumina (Al_2O_3), silicon carbide (SiC) or magnesia (MgO). Crystalline (i.e. non-amorphous) ceramics are typically have very high melting points (up to 2000 °C) and require firing (or sintering) in specialised furnaces. They are usually good electrical and thermal insulators (but not always), have relatively high strengths and stiffnesses and are usually brittle with a low fracture toughness.

Ceramics are processed into solid bodies, usually from fine, reacted (calcined) powder (typical grain size 1 μm) powders of the target ceramic composition (the so-called powder route). This involves adding an organic binder to the precursor powder before pressing into a compact or pre-form usually of circular or square cross-sectional geometry, known as a green body. This can be achieved either by uniaxial pressing in a die or by hot or cold isostatic pressing using a rubber mould, in which the pressure is applied uniformly from all directions. In this case the pressure is applied via either a liquid or gas medium. The green

body is then heat treated in a furnace to achieve densification and fusion of individual grains (which begin as discrete particles prior to sintering). The thermal process involves initially burning-out the binder by heating the green body to around 500°C and holding at this temperature for up to 1 hour. This process is often performed under flowing air to remove any hydro-carbons, water or gas produced via the burn-out process. Following burn-out, the body is heated to typically within 30% of its melting temperature, where densification takes place over a period of up to several hours. Finally the sintered sample is furnace-cooled to room temperature. Uniaxial pressing is used to produce green bodies of relatively simple geometry such as discs cylinders or cubes. Hot or cold isostatic pressing is used to produce green bodies of more complex geometries. Isostatic pressing tends to produce green bodies of higher density than uniaxial pressing (80% theoretical). [5]

(b) Individual atoms diffuse more rapidly during sintering at elevated temperature, which speeds-up the process of densification (the fusion of individual grains). This causes re-definition of grain boundaries as this fusion proceeds. The process of diffusion reduces the inter-grain porosity as sintering proceeds, which results in a decrease in sample volume. The grains increase in size with time, driven by the reduction in surface energy per unit volume for larger grains.

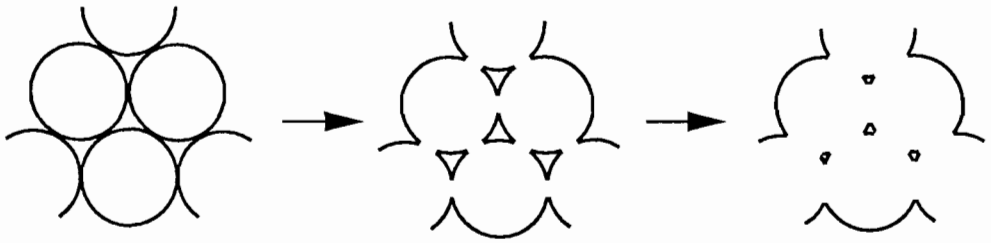

At a microscopic level, atoms diffuse from the grain boundaries between particles into the pores. Fine particles sinter much faster than coarse particles since the have a larger energy per unit volume, and hence a larger driving force for sintering, and the distances involved in diffusion are shorter.

Alternatively, liquid phase sintering can be used to produce a higher density ceramic. Here a small amount of additive such as MgO, Al_2O_3 or Si_3N_4, which reacts with the ceramic compound to form a lower melting point glass that wets and bonds the particles during sintering. Diffusion through the liquid is more rapid and the sintering is therefore faster. The presence of the glass phase, however, makes the ceramic unsuitable for operation at high temperature.

The diffusion-dependent sintering rate varies with temperature via the following equation;

$$\frac{d\rho}{dt} = \frac{C}{a^n} \exp\left(-\frac{Q}{RT}\right)$$

where ρ is the density, a is the particle size, C is a geometry-dependent constant, Q is the activation energy for sintering and $n \approx 3$.

The best mechanical properties (high stiffness and strength) are associated with high density (low porosity) and a low grain size. As a result, the initial grain size should be as small as possible and T should be close to the melting temperature, although melting should be avoided if the sample geometry is to be preserved. However, there is a trade-off between a high sintering temperature (which will promote grain growth) and a long sintering time (which will favour a high density). This represents a balance between grain

coalescence and growth. Additives can be added to inhibit grain growth during sintering, although these must not contaminate the target ceramic compound. [6]

(c) The strength of ceramics is determined by residual pores, due to incomplete sintering, and microcracks, due to thermal stress on cooling. These defects are similar in dimensions to the grain size. Hence their effect can be reduced by reducing the grain size of the ceramic by either reducing processing times (by HIPing) or by using a finer precursor powder (e.g. Al_2O_3 or MgO). Introducing second phase particles to the ceramic can also blunt cracks as they propagate and increase the fracture toughness of the ceramic (e.g. yttria-stabilised zirconia). Finally, transformation toughening can be used, which involves the structural transformation of a small region of secondary, stabilising phase material within the ceramic body. [4]

(d) Oxygen diffuses into the material from the top and sides, assuming that there is no significant oxygen diffusion through the support (although this does not affect the calculation). Thickness is the key length, given that the diffusion path to the centre from the edge is significantly greater. Assuming the 1-D diffusion equation; $D = D_0 \exp\left(\frac{-Q}{RT}\right)$

$$\frac{D_1}{D_2} = \frac{D_0 \exp\left(\frac{-Q}{RT_1}\right)}{D_0 \exp\left(\frac{-Q}{RT_2}\right)}$$

$$\ln\left(\frac{D_1}{D_2}\right) = \frac{Q}{R}\left(\frac{1}{T_2} - \frac{1}{T_1}\right) = -1.162 \text{ for } T_1 = 723 \text{ K and } T_2 = 773 \text{ K}$$

Therefore; $\frac{D_2}{D_1} \approx 3.2$

As a rule of thumb, diffusion distance with time, $x(t) = \sqrt{Dt}$, hence $t = \frac{x^2}{D}$.

In this case the diffusion distance is the same (1 cm), so $\frac{t_1}{t_2} = \frac{D_2}{D_1} \approx 3.2$.

Annealing at 450 °C takes approximately 3 times longer than at 500 °C. [5]

3. (a) *Suitable for casting*; A material that is suitable for shaping by a casting process. Applies to aluminium alloys close to the eutectic composition to achieve the necessary liquid "flow". These are usually non heat-treatable alloys such as Al-Si at the eutectic or near-eutectic composition (11.6 - 12 wt. % Al). Cast Al alloys are used for automotive parts (e.g. cylinder blocks) and domestic appliances (e.g. irons).

Wrought, heat-treatable; A material that is strengthened by a cold working process, such as rolling or beating, or by precipitate hardening. [Examples include the 2000-series (Al-Cu-Mg), 6000-series (Al-Mg-Si) and 7000-series (Al-Zn-Mg) alloys, although candidates are not expected to cite specific series]. Heat treatable alloys readily form a fine-scale precipitate at low temperatures (<200°C) from a supersaturated matrix. These coarsen by the formation of a series of phases to yield ultimately the equilibrium phase. As a result

the strength (hardness) of heat-treatable Al alloys is time-dependent. Heat-treatable Al alloys are usually quenched rapidly from T_0 to room temperature (T_1) to trap the alloying elements in a supersaturated solution. The alloy is then heated within the low temperature two phase region to T_2 to accelerate the thermally activated ageing process (during which the initial composition of the matrix, C_0, shifts to C_α). Heat-treatable Al alloys are used for car bodies, lightweight structures and ships and in aerospace engineering.

Wrought, non-heat-treatable; A material that is strengthened by a cold working process, such as rolling or beating, or by solid solution hardening. [Examples include the 1000-series, 3000-series (Al-Mn, Al-Mg-Mn) and 5000-series (Al-Mg) alloys, although candidates are not expected to cite specific series]. In contrast to heat-treatable alloys, the nucleation of a second phase in the supersaturated primary matrix is negligible at room temperature if the material is cooled via a moderate quench from a single phase state (this effectively beats the nose of the TTT diagram, which tends to be at relatively high temperature). Non-heat-treatable Al alloys are used for electrical conductors, beverage cans, saucepans, foil, tubes and lightweight ships.

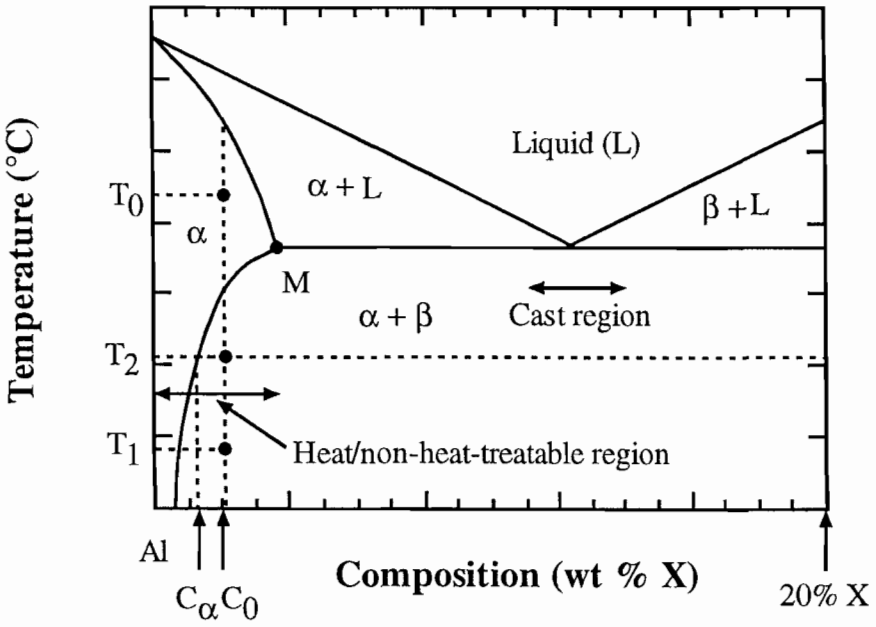

[6]

(b) The variation of yield stress or hardness with logarithm of ageing time (ageing curve) for a heat-treatable aluminium alloy at constant temperature is as follows;

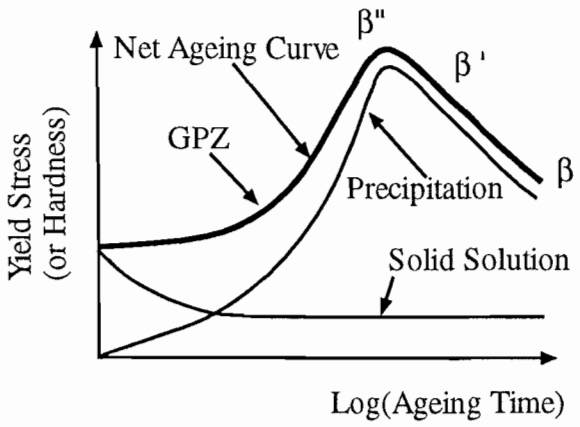

Solid solution hardening decreases as precipitates form from the supersaturated matrix.

The microstructure of the alloy evolves via the formation of a number of intermediate phases before the equilibrium phase is established, as follows;
Guinier-Preston (GP) zones or clusters form initially and homogeneously in large numbers in the form of thin discs of up to 100 atoms within the bulk of the grains. These precipitate out of the supersaturated solid solution to form small, coherent (crystallographic continuity at the phase boundary) particles in the bulk matrix. The precipitates then coarsen, driven by minimisation of the interface surface energy, which reduces their number but increases their average size and spacing. The particles pass through two transition, or intermediate phases before the equilibrium phase is established. The particles initially retain their coherency as they coarsen (β'' phase), but begin to lose coherency as they coarsen further (β' phase). Eventually the particle size becomes so large that all coherency is lost and the equilibrium phase is established (β phase).

The mechanism of hardening differs for coherent and incoherent precipitates. The former shear as the alloy deforms (i.e. in the slip plane of a dislocation). This involves breaking and re-forming a relatively large number of bonds, and hence is an effective mechanism of hardening (shear stress increases with the square root of the coherent particle radius). The resistance to dislocation motion changes as the precipitates become incoherent. In this case the half plane is pinned collectively by a line of particles, which do not deform as the dislocation passes (shear stress increases with the inverse of the incoherent particle radius). The peak in the ageing curve, therefore, occurs when there is a balance between shearing and by-passing (i.e. when a significant number of coherent particles are present and the distance between incoherent particles is still relatively small).

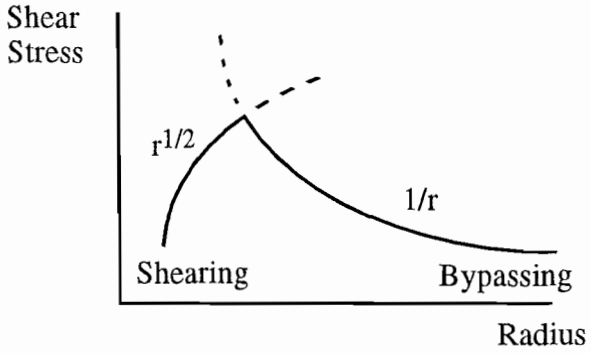

The maximum hardness usually coincides with the formation of the β' phase. Overaging occurs when the incoherent precipitates coarsen further, and their separation increases. This can be reversed by heating the alloy above the $\alpha/(\alpha + \beta)$ solvus line to re-dissolve the β phase and the second heat treatment repeated. [6]

(c) The microstructure contains a relatively large number of disc-shaped coherent particles of size around 50 nm that have coarsened from GP zones and a smaller number of larger incoherent particles. The latter also decorate the grain boundaries of the microstructure. This suggests that the alloy is mainly in the β'' phase, which places it close to the peak in the ageing curve.

E = 75 GPa, b = 0.3 nm.

From the Data Book; $\tau_y = \frac{c\,T}{b\,L}$, $T = \frac{1}{2} Gb^2$, $G \approx \frac{3}{8} E$ and $\sigma_y = 3\tau_y$, where T is the dislocation line tension and c is a constant (=2 in this case since the precipitates form 'strong obstacles').

Therefore, G = 28 GPa, $T = \frac{1}{2} 28 \times 10^9 \times (0.3 \times 10^{-9})^2 = 1.3 \times 10^{-9}$ N

$$\sigma_y = \frac{3\,c\,T}{b\,L} = \frac{3 \times 2 \times 1.3 \times 10^{-9}}{0.3 \times 10^{-9} \times 0.1 \times 10^{-6}} = \mathbf{260\ MPa}.$$ [6]

(d) (i) 2000 series aluminium alloy [e.g. Al-Cu(4.4%)-Mg(0.5%)] rivets precipitation harden at room temperature after quenching which decreases their ductility and makes them too hard. As a result, they need to be refrigerated prior to use to reduce the solid state diffusion rates and hence the degree of precipitate hardening.
(ii) 5000 series aluminium alloys [e.g. Al-Fe(0.7%)-Mg(1.5%)] are strengthened by cold working, not by heat treatment. Welding, therefore, will recrystallise the solid phase, annealing out any dislocations in the heat affected zone (HAZ). This can weaken the structure significantly and lead to its failure. [2]

4(a) The creep of metal alloys at low stresses occurs by diffusional flow, providing that the temperature is greater than about half the melting point of the alloy. In diffusional flow, atoms diffuse from grain boundaries perpendicular to the applied stress to grain boundaries normal to the applied stress, producing continuous elongation at a low overall strain rate. The overall rate depends on the rate of atomic diffusion, either along grain boundaries or through the bulk of the grains. [4]

(b) $\dot{\varepsilon} = \dot{\varepsilon_0} (\sigma / \sigma_0)^n = B\,\sigma^n$ at constant temperature and n.

Also $B = A \exp\left(\frac{-Q}{RT}\right)$, where Q is the activation energy and A is constant.

Therefore $\frac{\dot{\varepsilon_0}}{(\sigma_0)^n} = A \exp\left(\frac{-Q}{RT}\right)$ so $\sigma_0 = \frac{\dot{\varepsilon_0} \exp\left(\frac{Q}{RT}\right)^{\frac{1}{n}}}{A}$

$n \approx 3$ to 8 for a metal undergoing power law creep. [4]

(c) (i)

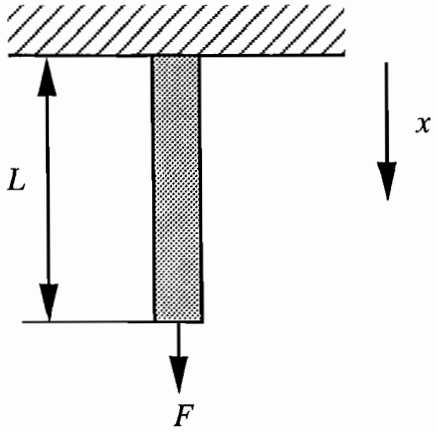

Cross-sectional area = A_0

$F = \rho\, g\, A_0\, (L - x)$

Stress at position x; $\sigma(x) = \frac{F}{A_0} = \rho\, g\, (L - x)$ $\qquad \dot{\varepsilon} = \frac{\dot{\varepsilon_0}}{\sigma_0^2} = \frac{\dot{\varepsilon_0}}{\sigma_0^2} \rho^2\, g^2\, (L - x)^2$

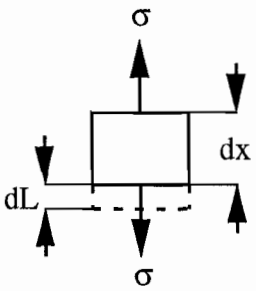

But, $\varepsilon = \frac{dL}{dx}$, hence $\qquad \dot{\varepsilon} = \frac{dL}{dx\, dt} = \frac{\dot{\varepsilon_0}}{\sigma_0^2} \rho^2\, g^2\, (L - x)^2$

$$\frac{dL}{dt} = \int_0^L \frac{\dot{\varepsilon_0}}{\sigma_0^2} \rho^2\, g^2\, (L - x)^2\, dx = \left[-\frac{1}{3} \frac{\dot{\varepsilon_0}}{\sigma_0^2} \rho^2\, g^2\, (L - x)^3 \right]_0^L = \frac{1}{3} \frac{\dot{\varepsilon_0}}{\sigma_0^2} \rho^2\, g^2\, L^3 \qquad [7]$$

(ii) $\rho = 19.3 \times 10^3$ kgm^{-3}, L = 0.1m and $\frac{\dot{\varepsilon_0}}{\sigma_0^2} = 2 \times 10^{-16}$ s^{-1}Pa^{-2} for tungsten in the power law creep regime with $n = 2$ at a working temperature of 2773 K.

$$\frac{dL}{L^3} = \frac{1}{3} \frac{\dot{\varepsilon_0}}{\sigma_0^2} \rho^2\, g^2\, dt$$

Need to calculate the time required for L to increase by 5%, either by integrating or (more approximately) simply by substituting numbers directly into the equation in part (c).

By integration;

$$t = \frac{3\,\sigma_0^2}{\dot{\varepsilon}_0\,\rho^2\,g^2}\int_L^{1.05L}\frac{dL}{L^3} = \frac{3\,\sigma_0^2}{2\,\dot{\varepsilon}_0\,\rho^2\,g^2\,L^2}\left(1-\frac{1}{1.05^2}\right)$$

$$= \frac{3\left(1-\frac{1}{1.05^2}\right)}{2\times 2\times 10^{-16}\times 19.3^2\times 10^6\times 9.8^2\times 10^{-2}} = 1.95\times 10^6\ \text{s} = \textbf{542 hours}$$

Direct calculation overestimates the time by around 13 hours (555 hours). Full marks providing approximate nature of answer is noted.

This is less than 1000 hours so the tungsten filament does not fulfil the design requirement. [5]

5(a) The neutral plane relates to the direction of friction and magnitude of velocity on the strip during the rolling process. Initially the roll periphery moves faster than the strip, as friction pulls it in. At the exit, however, the rolled strip moves faster than the periphery of the rolls due to continuity (i.e. since the thickness of the strip is reduced). As a result, the direction of friction stress acting on the material must necessarily reverse part way through the roll bite. The point at which the local friction stress on the material becomes zero and reverses, and which the peripheral velocity of the rolls becomes equal to that of the strip, therefore, is called the neutral plane. The pressure on the strip is maximum at the position of the neutral plane, in which case the normal stress on the strip resembles a forging friction hill (force per unit length for a wide strip).
Relationships between process variables;

For continuity; $h_1\,v_1 = h_2\,v_2$

Velocity of rolls = $\omega\,R$

At the input, in the region of the positive slope of the friction hill; $v_1 < \omega R$

At the output, in the region of the negative slope of the friction hill; $v_2 > \omega R$

At the peak of the friction hill (position of maximum roll force); $v_{strip} = \omega R$

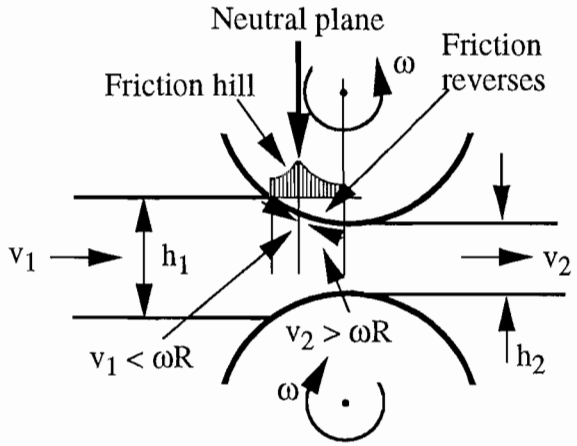

[5]

(b)(i) Friction is essential in the rolling process to draw the strip into the rolls. As a result neither the strip nor the rolls are lubricated during rolling (in contrast to the case of forging between platens).
(ii) A force applied through the axis of the rolls, normal to the plane of the strip is required to deform the strip.
(iii) The roll force P is given by the area under the friction hill (as with forging), but the line of action of the net force does not pass through the axis of the roll where the force P is applied. This produces a couple Q, which is the origin of the torque required to drive the strip through the roll bite.

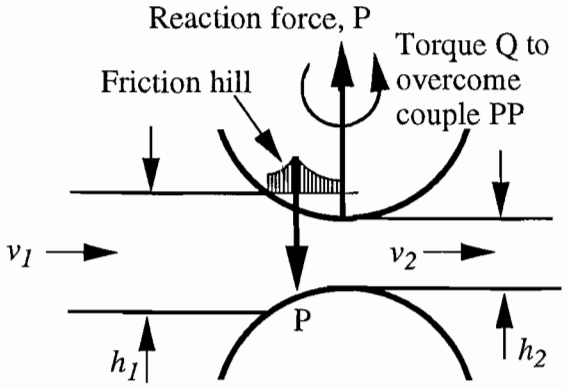

[6]

(c) Only one curve is required (note asymmetry of friction hill);

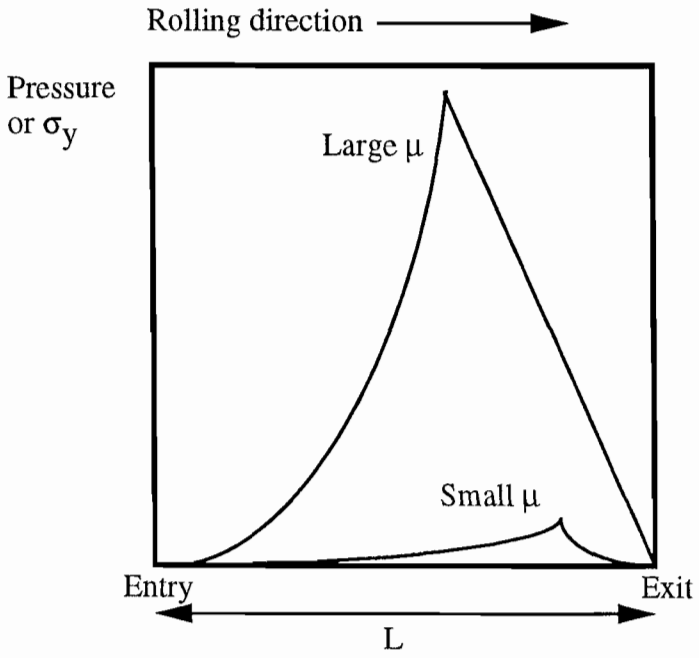

[4]

(d) A list of processing routes are given in Fig. 4.1a of the Materials Data Book. The candidate routes for the manufacture of high strength steel railway track are 1. shaped

rolling, 2. casting and 3. extrusion. The advantages and disadvantages of these routes are as follows;

1. Shaped rolling. This enables production of long lengths of railtrack with uniform cross-section and uniform mechanical properties. It is hot rolled and cooled slowly to produce a fine pearlite microstructure, which has the required mechanical strength. Good for section thicknesses up to 10 cm in batch quantities of thousands (Figs. 4.3 and 4.6 of the Data Book).
2. Casting. This enables the production of short lengths of track by a non-continuous process of relatively large mass and thickness (Figs. 4.2 and 4.3 of the Data Book). The rail track is subject to distortion on cooling and may need finishing by a secondary process. Cool rates and therefore microstructure less easy to control than shaped rolling. Sand casting is expensive (since it involves melting the steel) and does not generally yield relatively complex cross-sectional geometry in a reproducible way (low dimensional tolerance - Fig. 4.5 of the Data Book). Also low economic batch size (Fig. 4.6 Data Book).
3. Extrusion. This apparently enables production of lengths of railtrack with relatively uniform cross-section and uniform mechanical properties. Cool rates and microstructure relatively easy to control. Reasonable dimensional tolerance, large mass and thickness (Figs. 4.5, 4.2 and 4.3 of the Data Book) It is performed at elevated temperature, however, which leads to thermal distortion. Extrusion is not feasible for the production of large steel structures due to the large forces involved.

Shaped rolling is the preferred option [5]

6(a) Yield stress, or hardness, of plain carbon steels is determined primarily by (i) carbon content (i.e. alloying) and (ii) microstructure (i.e. secondary phase formation and the nature of the single-phase Fe-C solution). Microstructure is determined generally by cooling rate from the high temperature (723°C) austenite phase. Good candidates may sketch the increase in σ_y or hardness (and decrease in K_{1C} or ductility) with increasing carbon content. [Full marks for identifying factors (i) and (ii) with *brief* supporting discussion. The following gives more detail than required.]

Phase formation is determined primarily by solid state diffusion (thermally activated) of carbon atoms and undercooling in plain carbon steels. Practical processing is based on continuous cooling from the austenite phase with the rate of cooling determining diffusivity and hence the final phase composition of the steel. Plain carbon steels cooled rapidly from the austenite phase consist of martensite, which is a hard, meta-stable phase of iron. Martensite is then tempered to produce a range of target mechanical properties of the steel. Plain carbon steels cooled more slowly but at different rates contain different amounts of cementite (Fe_3C) which is a hard strong phase due to its high carbon content. The concentration and distribution of cementite, therefore, determines the hardness of the steel. Increasing the cooling rate of plain carbon steels from the austenite phase generally yields a finer distribution of cementite. Coarse pearlite (eutectoid ferrite and cementite), fine pearlite, upper bainite and lower bainite, for example, are produced by increasing the cooling rate. [5]

(b) Phases involved during cooling 0.8 wt.% carbon steel very slowly from 1000 °C to room temperature;

$T > 732°C$; austenite FCC (γ) single phase is present.

T < 732°C; a mixture of ferrite BCC (α phase) and cementite (Fe_3C) exists in the two phase region of the iron-carbide phase diagram shown in Fig. 6.3 of the Materials Data Book. 0.8% carbon content corresponds to the eutectoid composition, so slow cooling produces a coarse (since diffusion times are long), plate-like microstructure consisting of alternate α-phase and Fe_3C, known as pearlite;

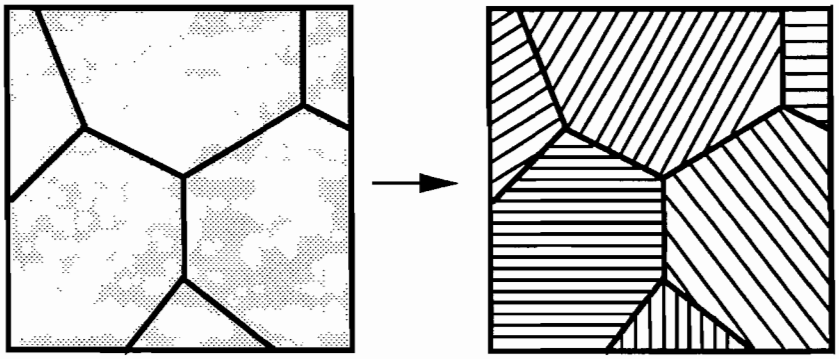

Austenite Pearlite (α + Fe_3C)

[5]

(c)

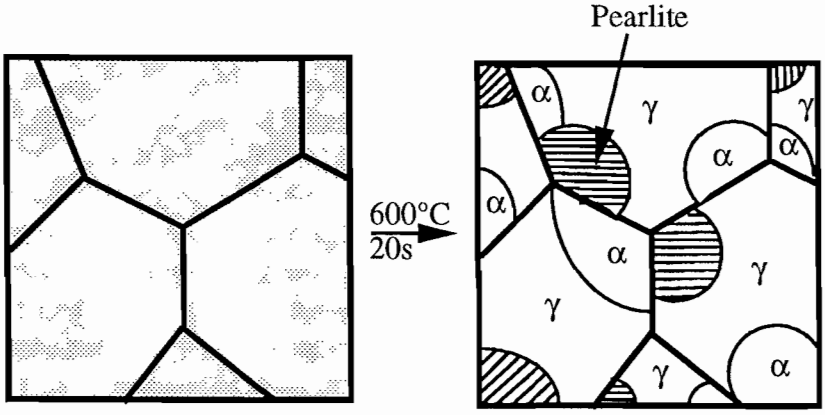

Austenite Austenite, pearlite + ferrite

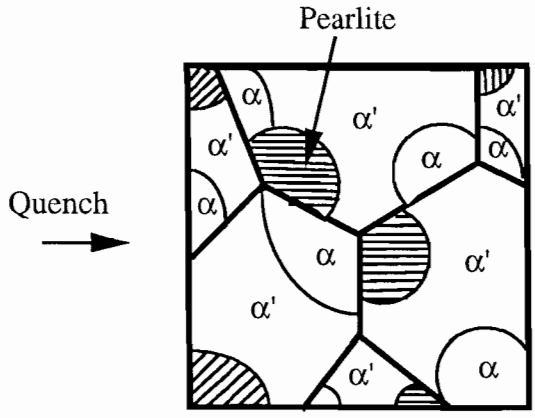

Martensite, pearlite + ferrite